Accuracy Assessment of the 2D Laminar Boundary Layer on a Flat Plate in an Immersed Boundary-Fourier Pseudospectral Simulations

Thiago F. S. de Freitas[1], Aristeu da Silveira Neto[1], Felipe P. Mariano[2]

[1]*Faculdade de Engenharia Mecânica (FEMEC), Universidade Federal de Uberlândia (UFU)*
Av. João Naves de Ávila - 2121 - Laboratório de Mecânica dos Fluidos - Bloco 5P, 38400-902, Minas Gerais, Brazil
thiago.santiago@ufu.br, aristeus@ufu.br
[2]*Escola de Engenharia Elétrica, Mecânica e da Computação (EMC), Universidade Federal de Goiás (UFG)*
Av. Esperança, s/n Campus Samambaia Al. Ingá, Prédio B5 Eng. Mecânica, 74.690-900, Goiás, Brazil
fpmariano@ufg.br

Abstract. We investigate the accuracy of the laminar boundary layer over a flat plate in the simulation by an immersed boundary – Fourier pseudospectral methods (IMERSPEC). In this study, we use the The Fourier pseudospectral method (FPM) combined with the Multi-Direct Forcing Method, can enforce the boundary conditions accurately by determining the body force iteratively. The IMERSPEC solves the continuity equation and linear momentum equations numerically implementing the Pseudospectral Fourier Method (PFM) with the use of the Discrete Fourier Transform (DFT), specifically the Fast Fourier Transform (FFT) algorithm. The reduced computational cost is achieved by the use of FFT as well as the pseudospectral approach which does not solve the convolution product of the advective term found in momentum linear equations. Furthermore, the mathematical process of pressure projection replaces the solution of Poisson Equation simultaneously ensures mass balance and decouples the pressure from the computational solution. The simulations of the laminar boundary layer on a flat plate at the Reynolds number of 10^4 are performed by using IMERSPEC and modelling the behaviour of the flow after the flat's leading edge to eliminate any undesirable Gibbs phenomenon. To obtain reasonably accurate results such that the maximum error from the friction coefficient distribution obtained is less than 4% over the useful domain we use at least a uniform mesh with 1024x256 collocation points. The rightness showed in these results indicates far improvement from the usual finite volume method's modelling which needs a local refinement mesh with far more volumes to present comparable results.

Keywords: Fourier Pseudospectral Method, Immersed Boundary Method, Multi Direct Forcing Method, 2D Laminar Boundary Layer over a Flat Plate.

1 Introduction

The methodology composed by Immersed Boundary Method (IBM) and Pseudospectral Fourier Method (PFM) called IMERSPEC was created by Mariano et al. [1] and since then has proved high order modelling. Although its significant accuracy this computational tool has been used solely in flows with only one non-periodic direction. This limitation occurs since all flows modelled by IMERSPEC must be periodic in all directions.

In an effort to maintain the methodology's high order and extend its application to non-periodic flows in all directions, it is modelled the laminar flow over a flat plate without pressure gradients. To the authors' knowledge, this is the first paper that models the classical Blasius flow by applying the Fourier method in all directions.

2 Methodology

This section presents the methods which are employed in the flow modelling, Pseudospectral Fourier Method (PFM) and Immersed Boundary Method (IBM), as the mathematical methodology and some strategies to perform

the modelling under a computational domain.

2.1 Mathematical Methodology

The present study uses continuity and Navier-Stokes equations in two-dimensional form to model the flow. Continuity equation is shown in Eq. 1,

$$\frac{\partial u_j}{\partial x_j} = 0, \tag{1}$$

where u_j is the flow velocity in m/s, x_j is space position in m to $j = 1$ and 2. The Eq. 2,

$$\frac{\partial u_i}{\partial t} + \frac{1}{2}\left[\frac{\partial (u_i u_j)}{\partial x_j} + u_j \frac{\partial u_i}{\partial x_j}\right] = -\frac{1}{\rho}\frac{\partial p}{\partial x_j} + \nu \frac{\partial^2 u_i}{\partial x_i \partial x_j} + f_i, \tag{2}$$

is implemented assuming a newtonian fluid and an isothermic flow with constant properties where t represents physical time in s, ρ is the fluid density in kg/m^3, p is the static pressure in N/m^2, ν is the fluid kinematic viscosity in m^2/s and f represents a source term, $kg/(m^2 \cdot s^2)$, divided for the fluid density, kg/m^3, thus resulting in m/s. Also, the advective term in Eq. 2 is written in the skew-symmetric form for computational stability.

2.2 Immersed Boundary Method

Immersed Boundary Method is implemented assuming two domains: an eulerian (Ω) and a lagrangian (Γ) one. In Ω, Eq. 1 and Eq. 2 are solved by PFM and in Γ, boundary conditions are imposed through immersed boundaries. It is assumed in this paper that variables written in lowercase belongs in Ω and variables in uppercase belongs in Γ.

To communicate between the domains, a source term is used. Thus, the f_i from Eq. 2 is defined in Eq. 3,

$$f_i(x_i, t) = \begin{cases} F(X_i, t) & \textit{if } x_i = X_i \\ 0 & \textit{otherwise} \end{cases}. \tag{3}$$

The source term represents the influence of the immersed boundary geometry into the flow, thus $f_i(x_i, t)$ is different than zero only in the interface between the immersed body and the fluid flow. In the present work, the lagrangian and eulerian mesh are coincident therefore Eq. 3 is applied without necessary adaptations.

The Direct Forcing Method (DFM), Uhlmann [2], may be used to determine f_i. Equations 4,

$$f_i = \frac{\partial u_i}{\partial t} + \frac{1}{2}\left[\frac{\partial (u_i u_j)}{\partial x_j} + u_j \frac{\partial u_i}{\partial x_j}\right] + \frac{1}{\rho}\frac{\partial p}{\partial x_j} - \nu \frac{\partial^2 u_i}{\partial x_i \partial x_j}, \tag{4}$$

are obtained by rearranging Eq. 2 in Ω to isolate f_i. From the domain definitions, $\Gamma \subset \Omega$ alternatively Eq. 2 is obtained assuming the continuum hypothesis, hence Eq. 4 can be rewritten in Γ through Eq. 5,

$$F_i(X_i, t) = \frac{\partial U_i}{\partial t} + RHS_i, \tag{5}$$

where $RHS_i = \frac{1}{2}\left[\frac{\partial (U_i U_j)}{\partial X_j} + U_j \frac{\partial U_i}{\partial X_j}\right] + \frac{1}{\rho}\frac{\partial P}{\partial X_j} - \nu \frac{\partial^2 U_i}{\partial X_i \partial X_j}$.

For DFM explanations purposes, it is applied the Euler Time Advancement Method in Eq. 5 as can be seen in the Eq. 6,

$$F_i(X_i, t) = \frac{U_i^{t+\Delta t} - U_i^t}{\Delta t} + RHS_i, \tag{6}$$

and then a temporary parameter, U_i^*, is added and subtracted simultaneously, thus resulting in Eq. 7,

$$F_i(X_i, t) = \frac{U_i^{t+\Delta t} - U_i^* + U_i^* - U_i^t}{\Delta t} + RHS_i. \tag{7}$$

Equations 7 can be decomposed in a two equations system,

$$\frac{U_i^* - U_i^t}{\Delta t} + RHS_i = 0, \tag{8}$$

$$F_i(X_i, t) = \frac{U_{IB} - U_i^*}{\Delta t}, \tag{9}$$

which compose the DFM. The term U_{IB} corresponds to the desirable velocity imposed to the flow therefore this is an open variable since it value depends of the implemented condition.

Still under continuum hypothesis, Eq. 8 can be rewritten in Ω and used to determine estimated eulerian velocity u_i^*. After the calculation of u_i^*, this information is transmitted where there are coincident lagrangian and eulerian meshes, *i.e.*, $u_i^* = U_i^*$ where $x_i = X_i$ and 0 otherwise. Then the lagrangian source term, $F_i(X_i, t)$, is defined by U_i^* and U_{IB} through Eq. 8 and the resulting value is transmitted to Ω by Eq. 3. The velocity value, in the next time step, is obtained by Eq. 9.

$$u_i^{t+\Delta t} = u_i^* + f_i \Delta t. \tag{10}$$

Equations 10 are developed from Eq. 9 in Ω, The fluid velocity in the immersed boundary should be equal to the desirable value imposed, U_{IB}, however it is not the case since temporal/spatial discretizations processes and mass conservation. For better accuracy, DFM is substituted by the Multi-Direct Forcing Method (MDF) which turns the DFM in an iterative process until $u_i^{t+\Delta t} \to U_{IB}$ accordingly a predetermined criterion. The works of Wang et al. [3] and Mariano et al. [1] may be consulted to more details about this method.

2.3 Pseudospectral Fourier Method

Equations 1 and 2 are solved by the Pseudospectral Fourier Method (PFM). Through PFM these equations are solved in the physical and spectral space therefrom the pseudospectral term in PFM through the use of the Fourier transform and the inverse Fourier transform. By this approach, differential terms are solved in the spectral space allowing high precision meanwhile convolutions are avoided by solving vector's products in the physical space.

By applying Fourier Transform in the continuity equation, Eq. 1, there is Eq. 11,

$$ik_j \hat{u}_j = 0, \tag{11}$$

where $i = \sqrt{-1}$, k_j is the wavenumber and $\hat{u}_j$ is the spectral transformed velocity field j. Equation 11 shows the product between two vectors, k_j and $\hat{u}_j$, equals to zero therefore, by analytical geometry, it is assumed a orthogonal relationship between $\hat{u}_j$ and k_j. Consequently, it is defined a imaginary plane called π which is perpendicular to k_j and contains $\hat{u}_j$ as can be be seen in Fig. 1.

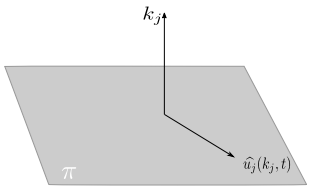

Figure 1. Continuity equation terms in spectral plane and the π plane.

After applying Fourier transform with its properties into Eq. 2, there is Eq. 12,

$$\frac{\partial \hat{u}_i}{\partial t} + \frac{1}{2}\left(ik_j \widehat{u_i u_j} + \hat{u}_j \frac{\partial \hat{u}_i}{\partial x_j} \right) = -ik_j \hat{p} - \nu k^2 \hat{u}_i + \hat{f}_i, \tag{12}$$

where k^2 is the square norm of the wave number, *i.e.*, $k^2 = k_i k_j$.

The change's rate of linear *momentum*, $\frac{\partial \hat{u}_i}{\partial t}$, belongs to the π plane as well as the viscous term, $\nu k^2 \hat{u}_i$ and since the pressure is a scalar variable, the pressure gradient term, $ik_i\hat{p}$, is collinear with vector k_j and thus perpendicular to the π plane. About the convective term and source term's positions in relation to this plane, nothing can be concluded. Equation 12 may be rewritten as Eq. 13,

$$\underbrace{\left(\frac{\partial}{\partial t} + \nu k^2 \hat{u}_i \right) \hat{u}_i}_{\in \pi} + \underbrace{\frac{1}{2}\left(ik_j \widehat{u_i u_j} + \hat{u}_j \frac{\partial \hat{u}_i}{\partial x_j} \right) + ik_j \hat{p} - \hat{f}_i}_{?} = 0, \tag{13}$$

to highlight its position's terms in relation to the π plane.

In Eq. 13 it is shown that the sum between the group of terms is null therefore, considering analytical geometry, both the groups are in the same plane, the π one. Since the convective, pressure and source terms' sum belong to the π plane, an operation called projection is applied. This mathematical operation is performed

by using a projection tensor concept which projects each term in the π plane and as the pressure gradient one is perpendicular to this plane, the projection operation decouples this term from the linear *momentum*'s solution. With the projection tensor applied on the second group in Eq. 13, it is obtained Eq. 14,

$$\frac{\partial \hat{u}_i}{\partial t} = -\nu k^2 \hat{u}_i + \varphi_{im}\left[\frac{1}{2}\left(ik_j\widehat{u_m u_j} + \hat{u}_j\frac{\partial \hat{u}_m}{\partial x_j}\right) - \hat{f}_m\right], \tag{14}$$

where $\varphi_{im} = \delta_{im} - \frac{kk_m}{k^2}$; $\delta_{im} = 1$ if $i = m$ and zero otherwise. Analysing the Eq. 14 is significant that the pressure decoupling turns the unknowns variables quantities values equals to the number of expressions and with the projection operation the continuity equation's properties in spectral space are always fulfilling mass conservation in the modelled flow.

2.4 Numerical-Computational Methodology

Mathematical functions as Fourier transform and inverse Fourier transform cannot be implemented in a numerical-computational application, therefore it is used the Discrete Fourier Transform (DFT) in the form of Fast Fourier Transform (FFT) an algorithm which enables the pseudospectral approach since its low computational cost.

Even though FFT turns possible PFM its use limit the IMERSPEC under two mainly aspects. The first one is mesh relatable, *i.e.*, the IMERSPEC's mesh must be uniform. The other limited aspect is due to the fact that all properties which would be transformed must have periodic boundary conditions (PBC).

To still model non-periodic boundary conditions (NPBC) of the flow, the computational domain is divided in two subsets: a complementary and useful domain or zones. In the useful domain, the desired flow is modelled and in the complementary zone, strategies are performed to turn the non-periodic flow in a periodic one.

To model the boundary layer flow on a flat plate, it is used the Fringe Method to turn periodic the non-periodic flow. This method was implemented in algorithms which employs MPF associated with other spatial high order method such as the Spectral Chebychev Method as can be seen in Nordström et al. [4], Lundbladh et al. [5] and Khujadze and Oberlack [6] and is imposed in Eq. 14 as a source term which may be seen in Eq. 15,

$$f_i = \Psi(u_i - Qtx_i), \tag{15}$$

where Ψ is a smooth dumping function different than zero only in the complementary domain and varies between 0 and 1; u_i are the flow velocity in t instant; and Qtx_i are desired target solutions in x_i direction. Figure 2a shows the Ψ used over the a complementary domain and the Qtx is represented by Fig. 2b.

(a) Ψ function

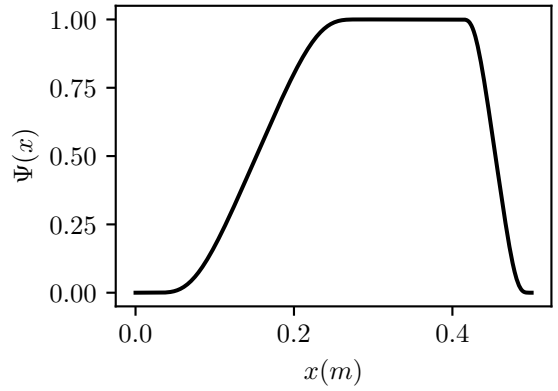

(b) Qtx

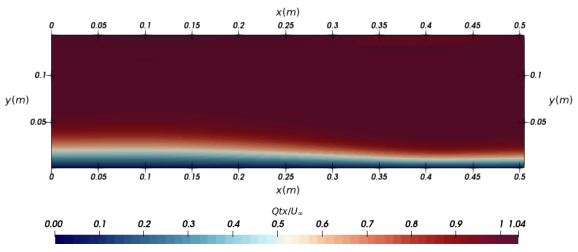

Figure 2. Fringe variables over a complementary domain

The dump function, Ψ, is smooth in the initial and final part of the complementary domain and it is defined as shown in Eq. 16

$$\Psi(x) = S\left(\frac{x - x_i}{\Delta_i}\right) - S\left(\frac{x - x_f}{\Delta_f} + 1\right), \tag{16}$$

where x_i and x_f mark the initial and final complementary zone's positions; Δ_i and Δ_f define Ψ form; and $S(x)$ is a smooth step function with $S(x) = 0$ for $x \leq 0$ and $S(x) = 1$ for $x \geq 1$. Qtx is variable over the direction of development's flow causing a fictitious spatial development inside the complementary zone, this parameter is defined by a $4/3$ Pade approximation of Blasius solution made by Ahmad and Al-Barakati [7] while Qty is defined by mass conservation.

Due to the use of a high order spatial discretization method as PFM, there must be implemented a high order temporal discretization method as well. In face of that, it is implemented in the present code the fourth-order 6 stages Runge-Kutta scheme (RK46) developed by Allampalli et al. [8].

3 Results and Discussion

In Figure 3 is shown the implementation's scheme of the two-dimensional boundary layer over a flat plate without pressure gradient. To avoid Gibbs phenomenon due the discontinuity of the leading edge's plate, the useful domain's inlet is imposed as the Blasius profiles u and v for $x = 0.5\,m$ using the Fringe Method.

Part of the transverse computational domain is not modelled to ensure the transverse FFT's periodicity condition while in x direction it is used the complementary domain to achieve this purpose. The dashed line in Fig. 3 marks where the periodicity conditions are imposed.

The top's boundary conditions are null Neumann conditions on the y direction while the plate's boundary conditions are the no slip ones. Both this boundary conditions are imposed by the IBM/MDF and as a shell concept to minimise flow's discontinuities as discussed by de Freitas [9].

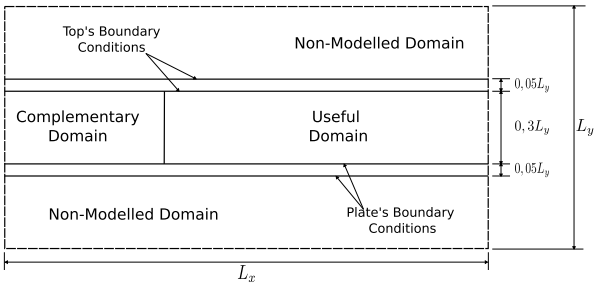

Figure 3. Boundary layer modelling's scheme

The parameters used in the virtual experiments are presented in Tab. 1 where L_y is the transverse computational domain's length, L_x is the longitudinal length, U_∞ is the free flow velocity, CFL represents the Courant-Friedrichs-Lewis temporal condition, t_f is the physical time modelled, ϵ is the MDF criterion and Re represents the Reynolds number calculated as viewed in Eq. 17,

$$Re = \frac{U_\infty \cdot x}{\nu}, \tag{17}$$

wherein $x = 1.0\,m$.

Table 1. Simulations parameters

L_y	L_x	U_∞	Re	CFL	t_f	ϵ
$0.38\,m$	$4L_y = 1.52\,m$	1.0 m/s	10^4	0.5	$10\,s$	10^{-4}

Virtual experiments were performed with meshes equal to 256×64, 512×128, 1024×256 and 2048×512 collocation points and the flow modelled is a laminar one.

Exact drag coefficients predictions, C_d, represents a sensible criterion to evaluate the methodology's accuracy according Hirsch [10]. In face of that, we use the friction coefficient, C_f, distribution along the useful domain to determine the accuracy of IMERSPEC comparing, when useful, the computational answers with Blasius solutions. The friction coefficients are chosen since the drag formed in a Blasius classical flow is composed solely by friction.

Figure 4a shows C_f distributions to the Blasius solution and the performed meshes while Fig. 4b presents the computational solutions' relative error in relation to Blasius. Both figures indicate that more accuracy is obtained

by mesh refinement mainly in the initial portion of the useful domain, $0.5 \leq x \leq 0.75\,m$, and part some final portion, $x \geq 1.3\,m$. This low rightness portions in the domain are, probably, due the fringe method which turns a non-periodic flow into a periodic one.

(a) C_f (b) Relative error

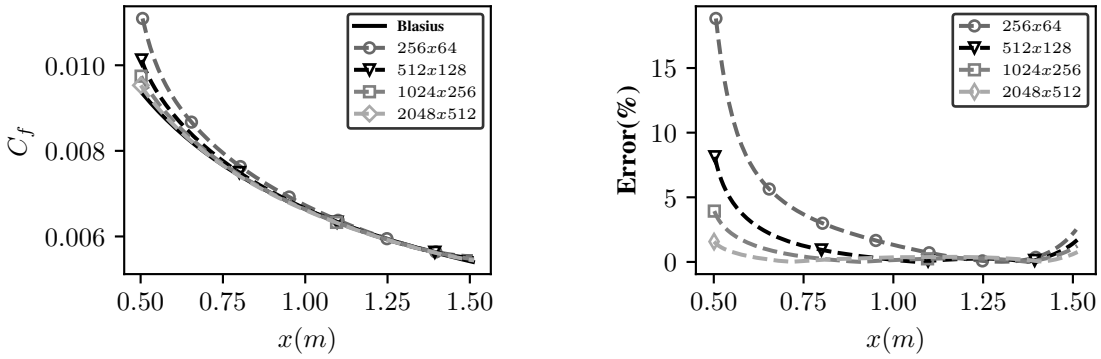

Figure 4. Friction coefficient and relative error distributions

The most refined mesh, 2048×512 collocation points, has, approximately, 2% maximum error which is a comparable result to commercial algorithms and is achieved by a uniform mesh. Also, the intermediate 1024×256 mesh presents comparable results with relative errors less than 4% over the useful domain.

Velocities u and v fields in the useful domain are viewed in Fig. 5a and 5b to the intermediate mesh of 1024×256 collocation points. The u field is shown to be qualitative close to the Blasius expected behaviour conversely the v field presents low accuracy close to the inlet's domain. Thus, in this paper the v component is more closely analysed.

(a) u (b) v

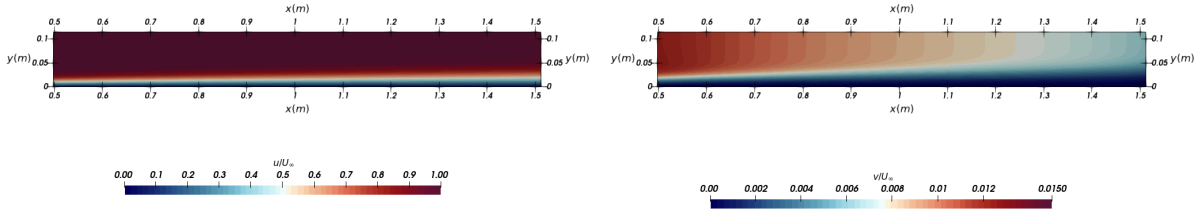

Figure 5. Field velocities in the useful domain to $1024x256$ collocation points

Horizontal v profiles in $L_y/2$ over all computational domain are shown in Fig. 6 where the complementary domain corresponds to $x < 0.5\,m$. It can be said that Qty, calculated by mass conservation, forces a negative value in v to recuperate the computational flow until the useful domain's inlet as a counterbalance to the fictitious spatial development imposed by Qtx, Fig. 2b. From Figure 6, is clear that the regions next to the fringe zone are the most inexact, as viewed in Fig. 4a, even though the mesh refinement causes significant improvement.

4 Conclusions

In this paper was modelled the flow over a flat plate without pressure gradient using the IMERSPEC. This classical flow was not adapted using pure Fourier Method or similar ones before since the flow must have PBC in all directions. The virtual experiment was possible due the use of the Fringe method and a transverse non modelled domain's part. It is highlighted that the most refined mesh, 2048×512, has relative errors less than 2% and the most computational solutions inaccuracy parts are close to the complementary domain.

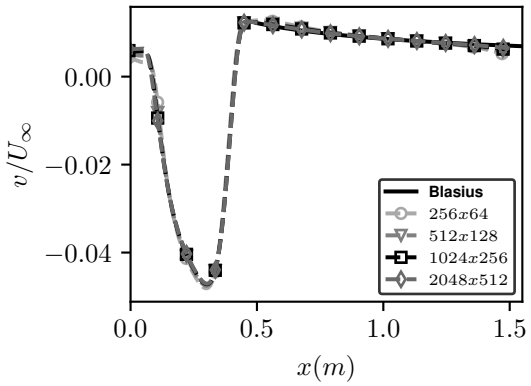

Figure 6. Horizontal v profile in $L_y/2$

Acknowledgements. The authors thank the Coordenação de Aperfeiçoamento de Pessoal de Nível Superior – Brasil (CAPES), the Faculdade de Engenharia Mecânica (FEMEC) of Universidade Federal de Uberlândia (UFU), the Escola de Engenharia Elétrica, Mecânica e de Computação (EMC) of the Universidade Federal de Goiás (UFG) for they support, FURNAS Centrais Elétricas and the "Programa de Pesquisa e Desenvolvimento Tecnológico" (P&D) of the ANEEL for the financial support.

Authorship statement. The authors hereby confirm that they are the sole liable persons responsible for the authorship of this work, and that all material that has been herein included as part of the present paper is either the property (and authorship) of the authors, or has the permission of the owners to be included here.

References

[1] F. P. Mariano, L. d. Q. Moreira, A. A. Nascimento, and A. Silveira. Neto. An improved immersed boundary method by coupling of the multi-direct forcing and fourier pseudo-spectral methods. *Journal of the Brazilian Society of Mechanical Sciences and Engineering*, vol. 44, n. 9. DOI:10.1007/s40430-022-03679-5, 2022.

[2] M. Uhlmann. An immersed boundary method with direct forcing for the simulation of particulate flows. *Journal of Computational Physics*, vol. 209, n. 2, pp. 448–476. DOI:10.1016/j.jcp.2005.03.017, 2005.

[3] Z. Wang, J. Fan, and K. Luo. Combined multi-direct forcing and immersed boundary method for simulating flows with moving particles. *International Journal of Multiphase Flow*, vol. 34, n. 3, pp. 283–302. DOI:10.1016/j.ijmultiphaseflow.2007.10.004, 2008.

[4] J. Nordström, N. Nordin, and D. Henningson. The fringe region technique and the fourier method used in the direct numerical simulation of spatially evolving viscous flows. *SIAM Journal on Scientific Computing*, vol. 20, n. 4, pp. 1365–1393. DOI:10.1137/s1064827596310251, 1999.

[5] A. Lundbladh, S. Berlin, M. Skote, C. Hildings, J. Choi, J. Kim, and D. S. Henningson. An efficient spectral method for simulation of incompressible flow over a flat plate. Technical report, Dept. of Mech., KTH, 1999.

[6] G. Khujadze and M. Oberlack. DNS and scaling laws from new symmetry groups of ZPG turbulent boundary layer flow. *Theoretical and Computational Fluid Dynamics*, vol. 18, n. 5, pp. 391–411. DOI:10.1007/s00162-004-0149-x, 2004.

[7] F. Ahmad and W. H. Al-Barakati. An approximate analytic solution of the blasius problem. *Communications in Nonlinear Science and Numerical Simulation*, vol. 14, n. 4, pp. 1021–1024. DOI:10.1016/j.cnsns.2007.12.010, 2009.

[8] V. Allampalli, R. Hixon, M. Nallasamy, and S. D. Sawyer. High-accuracy large-step explicit runge–kutta (HALE-RK) schemes for computational aeroacoustics. *Journal of Computational Physics*, vol. 228, n. 10, pp. 3837–3850. DOI:10.1016/j.jcp.2009.02.015, 2009.

[9] T. F. S. de Freitas. Modelagem matemática e computacional de camada limite laminar utilizando a metodologia mista pseudoespectral de fourier e fronteira imersa. Master's thesis, Universidade Federal de Uberlândia, Uberlândia. DOI:10.14393/ufu.di.2023.286, 2023.

[10] C. Hirsch. *Numerical computation of internal and external flows*, volume 01. Elsevier/Butterworth-Heinemann, Linacre House, Jordan Hill, Oxford OX2 8DP, 2nd edition, 2007.